Low-Frequency Acoustic Vibration Characteristics of Cylindrical Shells With Anisotropic Mechanical Material

Yin Danjie, Yan Xiaowei and Song Hao

CSSC Systems Engineering Research Institute, Beijing 100081, China. E-mail: 18518298281@163.com

Yi Kaijun

School of Aerospace Engineering, Beijing Institute of Technology, Beijing 100081, China.

Xiang Ping and Cui Zixian

CSSC Systems Engineering Research Institute, Beijing 100081, China.

(Received 21 April 2025; accepted 11 August 2025)

A precise acoustic vibration characteristic model of a cylindrical shell with anisotropic mechanical material was established based on three-dimensional elasticity theory and state space vector, and the accuracy of the analytical model was verified by comparing it with finite element results. By analogy with the concept of metamaterials, the modulus of the mechanical material is artificially changed to negative and complex numbers with extraordinary properties. Based on the acoustic vibration characteristic model, the influence of material parameters on the radiative noise transfer characteristics of anisotropic mechanical material cylindrical shells is studied.

1. INTRODUCTION

Thin-walled cylindrical shells are widely used in the main load-bearing structures of aerospace, underwater ships, transportation and other equipment. While meeting the static load-bearing capacity, they must also have good vibration and acoustic performance. At present, cylindrical shell structures mainly use viscoelastic damping materials to dissipate energy and reduce vibration noise. In the medium and high frequency bands, the elastic wave wavelength is small, and the viscoelastic damping material produces a large shear deformation, which has an outstanding vibration reduction and noise reduction effect. However, in the low frequency band, the elastic wave wavelength is large, and the viscoelastic damping material has a small deformation, resulting in little vibration reduction effect. In order to further improve the safety, reliability and service capability of equipment, it is urgent to develop new low-frequency vibration and noise reduction methods for cylindrical shell structures.

Fluid-loaded cylindrical shell structures usually use a viscoelastic damping layer to reduce their acoustic radiation. Lin[1] and Laulagnet et al.[2] studied the radiated acoustic power of a cylindrical shell with a damping layer in a flow field. The damping layer was simplified to a damping spring model, and its characteristics were characterized by complex stiffness. Laulagnet et al.[3] also studied the acoustic radiation of a cylindrical shell partially covered with viscoelastic damping material in a fluid. The radiated acoustic power and mean square velocity of the shell surface were calculated based on the Green function and modal expansion method. Through numerical analysis, it was found that selecting the appropriate damping layer stiffness can reduce the acoustic radiation of the composite shell in a wide frequency band. Cuschieri et al.[4] established a two-dimensional model of a cylindrical shell with a circumferential viscoelastic damping layer, ignoring the axial interaction. The study found that the circumferential modes of the shell are mutually coupled, and the edge of the viscoelastic damping layer will affect the radiated sound field. Heil et al.[5] also used a two-dimensional shell model to study the sound radiation of a cylindrical shell with an incompletely covered viscoelastic damping layer, considering the effect of the surrounding fluid domain on the viscoelastic damping layer, and found that when the covering gap is small, it will not significantly affect the radiation field unless the viscoelastic damping layer exhibits strong fluid-coupled oscillations at a specific frequency. Furthermore, Laulagnet et al.[6] established a more complex analytical model based on the three-dimensional Navier equation of the viscoelastic damping layer, taking into account the interaction forces in the circumferential, axial and radial directions, and studied the influence of more parameters such as the mass of the damping layer and the hydrostatic compression factor on the sound radiation. The results showed that the smaller the Young's modulus of the damping layer and the higher the analysis frequency, the more beneficial it is to vibration and noise reduction.

In addition, by analyzing the stiffness of the cylindrical shell, Ai Haifeng et al.[7] proposed increasing the local structural stiffness of the double-layer ribbed cylindrical shell, which has a significant effect on reducing the local vibration and low-frequency noise radiation of the underwater cylindrical shell structure. Xia Qiqiang et al.[8] added mass blocks to the ring ribs to form impedance enhancement components based on structural resistance enhancement technology. The results showed that adding a suitable mass block to the ring ribs close to the excitation source can effectively reduce the radiated sound power of the dominant mode of the cylindrical shell structure. Shen Shungen et al.[9] studied the coupling characteristics of the raft structure with viscoelastic damping

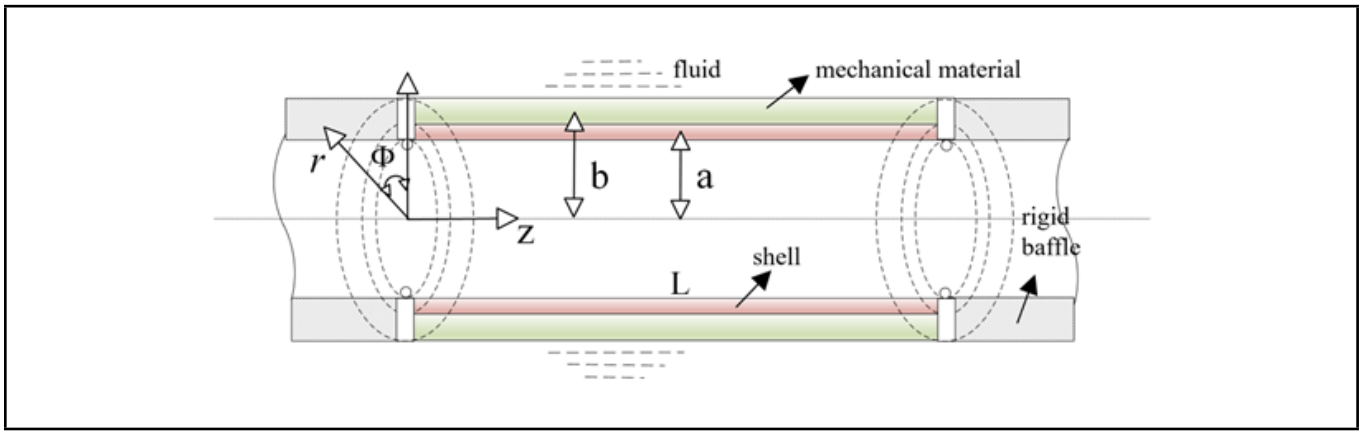

Figure 1. Schematic diagram of laying anisotropic mechanical material cylindrical shell model.

material and the acoustic medium, and reduced the acoustic radiation performance of the hull by designing a structure of upper vibration isolator-raft structure with viscoelastic material-lower vibration isolator-base hull-external flow field. Cao et al.[10] proposed a new active control method for the acoustic radiation of a cylindrical shell under axial excitation, using a pair of piezoelectric stack force actuators installed on the shell and parallel to the axial direction to reduce the acoustic radiation of the cylindrical shell structure.

At present, laying damping materials can effectively suppress the medium and high frequency vibrations of the structure, but the control effect on low frequency vibrations is minimal. Local resonance mechanical metamaterials have the ability to control large wavelength low frequency fluctuations, providing a new idea for low frequency vibration reduction and noise reduction of cylindrical shell structures. Local resonance mechanical metamaterials usually manifest as changes in material parameters. When the material parameters are negative, elastic waves become evanescent waves that cannot propagate within the frequency range of negative numbers. When the material parameters are complex numbers, the loss of elastic waves can be achieved, which achieves the purpose of vibration reduction and noise reduction. Therefore, this paper establishes an analytical model of the acoustic-vibration characteristics of a cylindrical shell with anisotropic mechanical materials, further introduces the design concept of metamaterials, changes the material parameters of the mechanical material to negative or complex numbers, and gives it extraordinary properties. It mechanistically verifies the possibility of metamaterial design for low-frequency vibration and noise reduction, and provides guidance for the realization of low-frequency elastic wave control of cylindrical shells.

2. ANALYTICAL MODELING

Based on the three-dimensional elastic theory and state space vector, the motion equation of the cylindrical shell laid with anisotropic mechanical materials was established. Then, combined with the force and displacement boundary conditions, the acoustic-vibration characteristic model of the cylindrical shell laid with anisotropic mechanical materials under fluid coupling was obtained. The calculation expressions of the sound power level are given to measure the sound radiation performance of the overall structure.

2.1. Laying Out the Equations of Motion for Cylindrical Shells Made of Anisotropic Mechanical Materials

Assume that the length of the cylindrical shell of anisotropic mechanical material is L, the radius of the shell section is a, the thickness is h, the radius of the mechanical material section is b, and the two ends are simply supported on semi-infinite rigid cylindrical baffles. The structure is placed in infinite water, as shown in Fig. 1. Traditional methods usually regard mechanical materials as fluid modeling, but they only consider the radial longitudinal wave effect of mechanical materials on the shell. In fact, the mechanical material has interaction forces on the shell in the radial, circumferential and axial directions. This is σ_{rr}, $\sigma_{r\phi}$, and σ_{rz}.

Therefore, the three-dimensional elastic equation is used to strictly describe the motion state of the mechanical material, and the relatively accurate Flügge shell theory is used to describe the motion of the cylindrical shell of the anisotropic mechanical material:

$$\begin{cases} L_{11}u + L_{12}v + L_{13}w = -\dfrac{1}{\rho_p c_p^2 h}\sigma_{rz}; \\ L_{21}u + L_{22}v + L_{23}w = -\dfrac{1}{\rho_p c_p^2 h}\sigma_{r\phi}; \\ L_{31}u + L_{32}v + L_{33}w = \dfrac{1}{\rho_p c_{\mathrm{p}}^2 h}(f + \sigma_{rr}); \end{cases} \tag{1}$$

in which ρ_p is the density of the fluid, $c_p = \sqrt{E/(\rho_p(1-\nu^2))}$ is the plane wave velocity, E and ν are the Young's modulus and Poisson's ratio of the shell, respectively, and f is the external excitation force. The coefficients of the equation of motion are:

$$L_{11} = \frac{\partial^2}{\partial z^2} + \frac{1-\nu}{2a^2}\frac{\partial^2}{\partial \phi^2} - \frac{1}{c_p^2}\frac{\partial^2}{\partial t^2} + \beta^2\frac{1-\nu}{2a^2}\frac{\partial^2}{\partial \phi^2};$$

$$L_{12} = \frac{1+\nu}{2a}\frac{\partial^2}{\partial \phi \partial z};$$

$$L_{13} = \frac{\nu}{a}\frac{\partial}{\partial z} - \beta^2 a\frac{\partial^3}{\partial z^3} + \beta^2\frac{1-\nu}{2a}\frac{\partial^3}{\partial \phi^2 \partial z};$$

$$L_{22} = \frac{1-\nu}{2}\frac{\partial^2}{\partial z^2} + \frac{1}{a^2}\frac{\partial^2}{\partial \phi^2} - \frac{1}{c_p^2}\frac{\partial^2}{\partial t^2} + \beta^2\frac{3(1-\nu)}{2}\frac{\partial^2}{\partial z^2};$$

$$L_{23} = \frac{1}{a^2}\frac{\partial}{\partial\phi} - \beta^2\frac{3-\nu}{2}\frac{\partial^3}{\partial\phi\partial z^2};$$
$$L_{33} = \frac{1}{a^2} + \beta^2\left(a^2\frac{\partial^4 w}{\partial z^4} + 2\frac{\partial^4 w}{\partial z^2\partial\phi^2} + \frac{1}{a^2}\frac{\partial^4 w}{\partial\phi^4}\right) + \frac{\beta^2}{a^2}\left(1 + 2\frac{\partial^2}{\partial\phi^2}\right) + \frac{1}{c_p^2}\frac{\partial^2}{\partial t^2}; \quad (2)$$

where $\beta = h^2/(12a^2)$. Based on the simply supported boundary conditions, the shell displacement can be expressed as follows in the form of mode superposition:

$$\begin{cases} u(\phi,z) = \sum_{\alpha=0}^{1}\sum_{n=0}^{\infty}\sum_{m=1}^{\infty} U_{nm}^{\alpha}\sin\left(n\phi + \frac{\alpha\pi}{2}\right)\cos k_m z; \\ v(\phi,z) = \sum_{\alpha=0}^{1}\sum_{n=0}^{\infty}\sum_{m=1}^{\infty} V_{nm}^{\alpha}\cos\left(n\phi + \frac{\alpha\pi}{2}\right)\sin k_m z; \\ w(\phi,z) = \sum_{\alpha=0}^{1}\sum_{n=0}^{\infty}\sum_{m=1}^{\infty} W_{nm}^{\alpha}\sin\left(n\phi + \frac{\alpha\pi}{2}\right)\sin k_m z; \end{cases} \quad (3)$$

in which U_{nm}^{α}, V_{nm}^{α}, W_{nm}^{α} are the modal expansion coefficients in three directions, $k_m = m\pi/L$ is the axial wave number, α is 0 or 1, representing the circumferential antisymmetric or symmetric mode, and $0 \le z \le L$. The displacement of the mechanical material and the force on the shell can also be written as the following modal superposition form:

$$\begin{cases} u_z = \sum_{\alpha=0}^{1}\sum_{n=0}^{\infty}\sum_{m=1}^{\infty} U_{nm}^{c\alpha}\sin\left(n\phi + \frac{\alpha\pi}{2}\right)\cos k_m z; \\ u_\phi = \sum_{\alpha=0}^{1}\sum_{n=0}^{\infty}\sum_{m=1}^{\infty} V_{nm}^{c\alpha}\cos\left(n\phi + \frac{\alpha\pi}{2}\right)\sin k_m z; \\ u_r = \sum_{\alpha=0}^{1}\sum_{n=0}^{\infty}\sum_{m=1}^{\infty} W_{nm}^{c\alpha}\sin\left(n\phi + \frac{\alpha\pi}{2}\right)\sin k_m z; \end{cases} \quad (4)$$

$$\begin{cases} \sigma_{rz} = \sum_{\alpha=0}^{1}\sum_{n=0}^{\infty}\sum_{m=1}^{\infty} F_{nm}^{\sigma z\alpha}\sin\left(n\phi + \frac{\alpha\pi}{2}\right)\cos k_m z; \\ \sigma_{r\phi} = \sum_{\alpha=0}^{1}\sum_{n=0}^{\infty}\sum_{m=1}^{\infty} F_{nm}^{\sigma\phi\alpha}\cos\left(n\phi + \frac{\alpha\pi}{2}\right)\sin k_m z; \\ \sigma_{rr} = \sum_{\alpha=0}^{1}\sum_{n=0}^{\infty}\sum_{m=1}^{\infty} F_{nm}^{\sigma r\alpha}\sin\left(n\phi + \frac{\alpha\pi}{2}\right)\sin k_m z. \end{cases} \quad (5)$$

Substituting Eqs. (3) and (5) into Eq. (1), according to the modal orthogonality, the motion equation of the cylindrical shell with anisotropic mechanical materials in the modal space can be obtained:

$$\begin{bmatrix} s_{11} & s_{12} & s_{13} \\ s_{21} & s_{22} & s_{23} \\ s_{31} & s_{32} & s_{33} \end{bmatrix}\begin{pmatrix} U_{nm}^{\alpha} \\ V_{nm}^{\alpha} \\ W_{nm}^{\alpha} \end{pmatrix} = \frac{1}{\rho_p c_p^2 h}\begin{pmatrix} 0 \\ 0 \\ F_{nm}^{\alpha} \end{pmatrix} + \frac{1}{\rho_p c_p^2 h}\begin{pmatrix} -F_{nm}^{\sigma z\alpha} \\ -F_{nm}^{\sigma\phi\alpha} \\ F_{nm}^{\sigma r\alpha} \end{pmatrix}. \quad (6)$$

The elements in the coefficient matrix are expressed as:

$$s_{11} = -k_m^2 - \frac{1-\nu}{2a^2}n^2 + \frac{\omega^2}{c_p^2} - \beta^2\frac{1-\nu}{2a^2}n^2;$$
$$s_{12} = -\frac{1+\nu}{2a}nk_m;$$
$$s_{13} = \frac{\nu}{\alpha}k_m + \beta^2 a k_m^3 - \beta^2\frac{1-\nu}{2a}n^2 k_m;$$
$$s_{22} = -\frac{1-\nu}{2}k_m^2 - \frac{n^2}{a^2} + \frac{\omega^2}{c_p^2} - \beta^2\frac{3(1-\nu)}{2}k_m^2;$$
$$s_{23} = \frac{n}{a^2} + \beta^2\frac{3-\nu}{2}nk_m^2;$$
$$s_{33} = \frac{1}{a^2} + \beta^2\left(a^2k_m^4 + 2n^2k_m^2 + \frac{n^4}{a^2}\right) + \frac{\beta^2}{a^2}(1-2n^2) - \frac{\omega^2}{c_p^2};$$
$$s_{21} = s_{12}; \quad s_{31} = -s_{13}; \quad s_{32} = -s_{23}. \quad (7)$$

The modal coefficient F_{nm}^{α} can be obtained based on the modal orthogonality of the external excitation force $f(\varphi, z)$. Assuming that there is a radial concentrated excitation force with a value of f_0 at the surface (φ_0, z_0) of the cylindrical shell, the expression is:

$$f(\phi,z) = \frac{f_0}{a}\delta(\phi-\phi_0)\delta(z-z_0). \quad (8)$$

Then its modal coefficient can be written as:

$$F_{nm}^{\alpha} = \begin{cases} \frac{2}{\pi a L}f_0\sin\left(n\phi_0 + \frac{\alpha\pi}{2}\right)\sin(k_m z_0), & \alpha = 0; \\ \frac{\varepsilon_n}{\pi a L}f_0\sin\left(n\phi_0 + \frac{\alpha\pi}{2}\right)\sin(k_m z_0), & \alpha = 1; \end{cases} \quad (9)$$

in which, when $n = 0$, it is $\varepsilon_n = 1$, when $n \ne 0$, it is $\varepsilon_n = 2$, and the corresponding F_{nm}^{α} of other forms of excitation force can be calculated similarly.

2.2. Establishing the Transfer Relationship Between Mechanical Materials and Shells Based on State Space Vectors

The interaction force in Eq. (6) can be obtained from the stress relationship in the structure. The constitutive relationship of orthotropic mechanical materials in the cylindrical coordinate system can be expressed as:

$$\begin{Bmatrix} \sigma_{rr} \\ \sigma_{\phi\phi} \\ \sigma_{zz} \\ \sigma_{\phi z} \\ \sigma_{rz} \\ \sigma_{r\phi} \end{Bmatrix} = \begin{bmatrix} C_{11} & C_{12} & C_{13} & 0 & 0 & 0 \\ C_{12} & C_{22} & C_{23} & 0 & 0 & 0 \\ C_{13} & C_{23} & C_{33} & 0 & 0 & 0 \\ 0 & 0 & 0 & C_{44} & 0 & 0 \\ 0 & 0 & 0 & 0 & C_{55} & 0 \\ 0 & 0 & 0 & 0 & 0 & C_{66} \end{bmatrix}\begin{Bmatrix} \varepsilon_{rr} \\ \varepsilon_{\phi\phi} \\ \varepsilon_{zz} \\ 2\varepsilon_{\phi z} \\ 2\varepsilon_{rz} \\ 2\varepsilon_{r\phi} \end{Bmatrix}. \quad (10)$$

In the small deformation assumption, the structural geometric relationship in the cylindrical coordinate system is:

$$\varepsilon_{rr} = \frac{\partial u_r}{\partial r}; \quad \varepsilon_{\phi\phi} = \frac{1}{r}\frac{\partial u_\phi}{\partial\phi} + \frac{u_r}{r}; \quad \varepsilon_{zz} = \frac{\partial u_z}{\partial z};$$
$$2\varepsilon_{r\phi} = \frac{1}{r}\frac{\partial u_r}{\partial\phi} + \frac{\partial u_\phi}{\partial r} - \frac{u_\phi}{r};$$
$$2\varepsilon_{rz} = \frac{\partial u_r}{\partial z} + \frac{\partial u_z}{\partial r}; \quad 2\varepsilon_{\phi z} = \frac{\partial u_\phi}{\partial z} + \frac{\partial u_z}{r\partial\phi}; \quad (11)$$

in which u_i, σ_{ij}, and ε_{ij} represent the displacement, stress and strain of the mechanical material respectively, and C_{ij} represents the elastic constant of the medium.

Substituting Eq. (11) into Eq. (10) yields the relationship between stress and strain of mechanical materials:

$$\begin{aligned}
\sigma_{rr} &= C_{11}\frac{\partial u_r}{\partial r} + C_{12}\left(\frac{1}{r}\frac{\partial u_\phi}{\partial \phi} + \frac{u_r}{r}\right) + C_{13}\frac{\partial u_z}{\partial z};\\
\sigma_{\phi\phi} &= C_{12}\frac{\partial u_r}{\partial r} + C_{22}\left(\frac{1}{r}\frac{\partial u_\phi}{\partial \phi} + \frac{u_r}{r}\right) + C_{23}\frac{\partial u_z}{\partial z};\\
\sigma_{zz} &= C_{13}\frac{\partial u_r}{\partial r} + C_{23}\left(\frac{1}{r}\frac{\partial u_\phi}{\partial \phi} + \frac{u_r}{r}\right) + C_{33}\frac{\partial u_z}{\partial z};\\
\sigma_{\phi z} &= C_{44}\left(\frac{\partial u_\phi}{\partial z} + \frac{\partial u_z}{r\partial \phi}\right);\\
\sigma_{rz} &= C_{55}\left(\frac{\partial u_r}{\partial z} + \frac{\partial u_z}{\partial r}\right);\\
\sigma_{r\phi} &= C_{66}\left(\frac{1}{r}\frac{\partial u_r}{\partial \phi} + \frac{\partial u_\phi}{\partial r} - \frac{u_\phi}{r}\right).
\end{aligned} \tag{12}$$

Under the condition of no body force, the equilibrium equation of the body force of the mechanical material unit is:

$$\begin{aligned}
&\frac{\partial \sigma_{rr}}{\partial r} + \frac{1}{r}\frac{\partial \sigma_{r\phi}}{\partial \phi} + \frac{\partial \sigma_{rz}}{\partial z} + \frac{\sigma_{rr}-\sigma_{\phi\phi}}{r} = \rho\frac{\partial^2 u_r}{\partial t^2};\\
&\frac{\partial \sigma_{r\phi}}{\partial r} + \frac{1}{r}\frac{\partial \sigma_{\phi\phi}}{\partial \phi} + \frac{\partial \sigma_{\phi z}}{\partial z} + \frac{2\sigma_{r\phi}}{r} = \rho\frac{\partial^2 u_\phi}{\partial t^2};\\
&\frac{\partial \sigma_{rz}}{\partial r} + \frac{1}{r}\frac{\partial \sigma_{\phi z}}{\partial \phi} + \frac{\partial \sigma_{zz}}{\partial z} + \frac{\sigma_{rz}}{r} = \rho\frac{\partial^2 u_z}{\partial t^2}.
\end{aligned} \tag{13}$$

Substituting Eqs. (4) and (5) into Eqs. (12) and (13), we can obtain:

$$\begin{aligned}
\frac{\partial U_{nm}^{c\alpha}}{\partial r} &= \frac{1}{C_{55}}F_{nm}^{\sigma z\alpha} + ik_m W_{nm}^{c\alpha};\\
\frac{\partial V_{nm}^{c\alpha}}{\partial r} &= \frac{1}{C_{66}}F_{nm}^{\sigma\phi\alpha} + \frac{1}{r}V_{nm}^{c\alpha} - \frac{in}{r}W_{nm}^{c\alpha};\\
\frac{\partial W_{nm}^{c\alpha}}{\partial r} &= \frac{1}{C_{11}}F_{nm}^{\sigma r\alpha} + \frac{ik_m C_{13}}{C_{11}}U_{nm}^{c\alpha} - \frac{inC_{12}}{rC_{11}}V_{nm}^{c\alpha} -\\
&\quad \frac{C_{12}}{rC_{11}}W_{nm}^{c\alpha};\\
\frac{\partial F_{nm}^{\sigma z\alpha}}{\partial r} &= \frac{iC_{13}k_m}{C_{11}}F_{nm}^{\sigma r\alpha} - \frac{1}{r}F_{nm}^{\sigma z\alpha} +\\
&\quad \left(\frac{n^2C_{44}}{r^2} + k_m^2C_{33} - \rho\omega^2 - \frac{k_m^2C_{13}^2}{C_{11}}\right)U_{nm}^{c\alpha} +\\
&\quad \left(\frac{nk_mC_{12}C_{13}}{rC_{11}} - \frac{nk_m}{r}(C_{44}+C_{22})\right)V_{nm}^{c\alpha} +\\
&\quad \left(\frac{ik_mC_{22}}{r} - \frac{ik_mC_{12}C_{13}}{rC_{11}}\right)W_{nm}^{c\alpha};\\
\frac{\partial F_{nm}^{\sigma\phi\alpha}}{\partial r} &= -\frac{inC_{12}}{rC_{11}}F_{nm}^{\sigma r\alpha} - \frac{2}{r}F_{nm}^{\sigma\phi\alpha} +\\
&\quad \left(\frac{nk_mC_{12}C_{13}}{rC_{11}} - \frac{nk_m}{r}(C_{23}+C_{44})\right)U_{nm}^{c\alpha} +\\
&\quad \left(\frac{n^2C_{22}}{r^2} - \frac{n^2C_{12}^2}{r^2C_{11}} + C_{44}k_m^2 - \rho\omega^2\right)V_{nm}^{c\alpha} +\\
&\quad \left(\frac{inC_{12}^2}{r^2C_{11}} - \frac{inC_{22}}{r^2}\right)W_{nm}^{c\alpha};\\
\frac{\partial F_{nm}^{\sigma r\alpha}}{\partial r} &= -\frac{in}{r}F_{nm}^{\sigma\phi\alpha} + ik_mF_{nm}^{\sigma z\alpha} + \left(\frac{C_{12}}{rC_{11}} - \frac{1}{r}\right)F_{nm}^{\sigma r\alpha} +\\
&\quad \left(\frac{ik_mC_{12}C_{13}}{rC_{11}} - \frac{ik_mC_{23}}{r}\right)U_{nm}^{c\alpha} +\\
&\quad \left(\frac{inC_{22}}{r^2} - \frac{inC_{12}^2}{r^2C_{11}}\right)V_{nm}^{c\alpha} +\\
&\quad \left(\frac{C_{22}}{r^2} - \rho\omega^2 - \frac{C_{12}^2}{r^2C_{11}}\right)W_{nm}^{c\alpha}.
\end{aligned} \tag{14}$$

Assume the state vectors of stress and displacement are:

$$\begin{aligned}
\mathbf{D}(r) = \big\{&U_{nm}^{c\alpha}(r), V_{nm}^{c\alpha}(r), W_{nm}^{c\alpha}(r), F_{nm}^{\sigma z\alpha}(r),\\
&F_{nm}^{\sigma\phi\alpha}(r), F_{nm}^{\sigma r\alpha}(r)\big\}^T
\end{aligned} \tag{15}$$

According to the constitutive relationship and geometric relationship of the material in the cylindrical coordinate system, substituting it into the state space Eq. (15), the ordinary differential equation can be expressed as:

$$\frac{d}{dr}\mathbf{D}(r) = \mathbf{P}(r)\mathbf{D}(r); \tag{16}$$

in the formula, the matrix $\mathbf{P}(r)$ can be written as Eq. (17).

The state space vectors of the shell and mechanical materials are expressed in the form of exponential solutions:

$$\mathbf{D}(r_a) = e^{(r_a-r_b)\mathbf{P}\left(\frac{r_a+r_b}{2}\right)}\mathbf{D}(r_b). \tag{18}$$

Assuming $e^{(r_a-r_b)\mathbf{P}(\frac{r_a+r_b}{2})} = \begin{bmatrix}\mathbf{T}_{11} & \mathbf{T}_{12}\\ \mathbf{T}_{21} & \mathbf{T}_{22}\end{bmatrix}$, $\mathbf{T}_{ij}$ is a 3×3 matrix, we can get the transfer relationship between the mechanical material and the shell:

$$\begin{Bmatrix} U_{nma}^{\alpha}\\ V_{nma}^{\alpha}\\ W_{nma}^{\alpha}\\ F_{nma}^{\sigma z\alpha}\\ F_{nma}^{\sigma\phi\alpha}\\ F_{nma}^{\sigma r\alpha}\end{Bmatrix} = \begin{bmatrix}\mathbf{T}_{11} & \mathbf{T}_{12}\\ \mathbf{T}_{21} & \mathbf{T}_{22}\end{bmatrix}\begin{Bmatrix} U_{nmb}^{c\alpha}\\ V_{nmb}^{c\alpha}\\ W_{nmb}^{c\alpha}\\ F_{nmb}^{\sigma z\alpha}\\ F_{nmb}^{\sigma\phi\alpha}\\ F_{nmb}^{\sigma r\alpha}\end{Bmatrix}. \tag{19}$$

2.3. Continuity Boundary Conditions on Contact Surfaces of Anisotropic Mechanical Materials

The boundary conditions of mechanical material motion are analyzed below. At the interface between the shell and the mechanical material ($r = a$), the continuity conditions of the displacement of the mechanical material and the shell are met, and in the modal space, there are:

$$W_{nm}^{c\alpha}\,|_{r=a} = W_{nm}^{\alpha};\quad V_{nm}^{c\alpha}\,|_{r=a} = V_{nm}^{\alpha};\quad U_{nm}^{c\alpha}\,|_{r=a} = U_{nm}^{\alpha}. \tag{20}$$

At the interface between mechanical material and fluid ($r = b$), the boundary conditions of stress continuity and displacement continuity are met, and the following relationship holds in the modal space:

$$\begin{aligned}
&F_{nm}^{\sigma r\alpha}\,|_{r=b} = -P_{nm}^{f\alpha}\,|_{r=b};\qquad F_{nm}^{\sigma\phi\alpha}\,|_{r=b} = 0;\\
&F_{nm}^{\sigma z\alpha}\,|_{r=b} = 0;\qquad W_{nm}^{c\alpha}\,|_{r=b} = W_{nm}^{f\alpha}\,|_{r=b};
\end{aligned} \tag{21}$$

the sound pressure amplitude is expressed as:

$$P_{nmb}^{f\alpha} = \dot{W}_{nmb}^{f\alpha}Z_{nmm} = -i\omega W_{nmb}^{f\alpha}Z_{nmm}; \tag{22}$$

$$\mathbf{P}(r)=\begin{bmatrix} 0 & 0 & -k_m & \frac{1}{C_{55}} & 0 & 0 \\ 0 & \frac{1}{r} & -\frac{n}{r} & 0 & \frac{1}{C_{66}} & 0 \\ \frac{k_m C_{13}}{C_{11}} & \frac{nC_{12}}{rC_{11}} & -\frac{C_{12}}{rC_{11}} & 0 & 0 & \frac{1}{C_{11}} \\ \frac{n^2C_{44}}{r^2}+k_m^2C_{33}-\rho\omega^2-\frac{k_m^2C_{13}^2}{C_{11}} & \frac{nk_m}{r}\left(C_{44}+C_{23}-\frac{C_{12}C_{13}}{C_{11}}\right) & \frac{k_mC_{12}C_{13}}{rC_{11}}-\frac{k_mC_{23}}{r} & -\frac{1}{r} & 0 & -\frac{k_mC_{13}}{C_{11}} \\ \frac{nk_m}{r}\left(C_{44}+C_{23}-\frac{C_{12}C_{13}}{C_{11}}\right) & \frac{n^2C_{22}}{r^2}-\frac{n^2C_{12}^2}{r^2C_{11}}+C_{44}k_m^2-\rho\omega^2 & \frac{nC_{12}^2}{r^2C_{11}}-\frac{nC_{22}}{r^2} & 0 & -\frac{2}{r} & \frac{nC_{12}}{rC_{11}} \\ \frac{k_mC_{12}C_{13}}{rC_{11}}-\frac{k_mC_{23}}{r} & \frac{nC_{12}^2}{r^2C_{11}}-\frac{nC_{22}}{r^2} & \frac{C_{22}}{r^2}-\rho\omega^2-\frac{C_{12}^2}{r^2C_{11}} & k_m & \frac{n}{r} & \frac{C_{12}}{rC_{11}}-\frac{1}{r} \end{bmatrix} \tag{17}$$

in which Z_{nmm} is the acoustic radiation impedance of the mechanical material surface, which can be expressed as follows:

$$Z_{nmm}=\begin{cases} \dfrac{2\rho cbmm\pi^2}{\varepsilon_n k_c^3L^2}\displaystyle\int_0^{\infty}\frac{Z_n(\gamma)}{\sqrt{1-\chi^2}}\frac{N_{nm}(\chi)}{(\chi^2-(\frac{m\pi}{k_cL})^2)^2}d\chi, \\ \qquad\qquad 0<\chi<1; \\ \dfrac{2\rho cbmm\pi^2}{\varepsilon_n k_c^3L^2}\displaystyle\int_0^{\infty}\frac{Z_n(\gamma)}{\sqrt{1-\chi^2}}\frac{N_{nm}(\chi)}{(\chi^2-(\frac{m\pi}{k_cL})^2)^2}d\chi, \\ \qquad\qquad \chi>1; \end{cases} \tag{23}$$

$$N_{nm}(\chi)=\begin{cases} 4\cos^2\dfrac{k_cL\chi}{2}, & m \text{ is an odd number;} \\ 4\sin^2\dfrac{k_cL\chi}{2}, & m \text{ is an even number;} \end{cases} \tag{24}$$

in which $k_c=\omega/c=\sqrt{k_x^2+(\gamma/R)^2}$ is the number of sound waves in the fluid, variable $\chi=k_x/k_c$, then $\gamma=k_cR\sqrt{1-\chi^2}$, $k_r=\gamma/R=k_c\sqrt{1-\chi^2}$, $Z_n(\gamma)=iH_n^{(1)}(\gamma)/H_n^{(1)'}(\gamma)$, $H_n^{(1)}$ represents the first-order n-th Hankel function, ρc is the wave impedance in the infinite fluid medium, and c represents the speed of sound waves in the fluid. For a given ω, k_x can only be a real number or an imaginary number.

When $0<\chi<1$, that is $k_x<k_c$, γ and k_r are both real numbers, the sound wave propagates in the form of traveling waves. From the recursive formula, we can get:

$$\begin{aligned} H_n^{(1)}(\gamma)&=J_n(\gamma)+iY_n(\gamma); \\ H_n^{(1)'}(\gamma)&=\frac{1}{2}\left[H_{n-1}^{(1)}(\gamma)-H_{n+1}^{(1)}(\gamma)\right]. \end{aligned} \tag{25}$$

Therefore, $Z_n(\gamma)$ in Eq. (23) can be written as:

$$Z_n(\gamma)=\frac{iH_n^{(1)}(\gamma)}{H_n^{(1)'}(\gamma)}=\theta_n(\gamma)-i\zeta_n(\gamma); \tag{26}$$

in which:

$$\theta_n(\gamma)=\frac{2J_n(\gamma)[Y_{n-1}(\gamma)-Y_{n+1}(\gamma)]-Y_n(\gamma)[J_{n-1}(\gamma)-J_{n+1}(\gamma)]}{[J_{n-1}(\gamma)-J_{n+1}(\gamma)]^2+[Y_{n-1}(\gamma)-Y_{n+1}(\gamma)]^2}; \tag{27}$$

$$\zeta_n(\gamma)=\frac{-2J_n(\gamma)[J_{n-1}(\gamma)-J_{n+1}(\gamma)]+Y_n(\gamma)[Y_{n-1}(\gamma)-Y_{n+1}(\gamma)]}{[J_{n-1}(\gamma)-J_{n+1}(\gamma)]^2+[Y_{n-1}(\gamma)-Y_{n+1}(\gamma)]^2}. \tag{28}$$

When $\chi>1$, that is $k_x>k_c$, $\gamma=i\delta$ and k_r are imaginary numbers, the sound wave degenerates into an attenuated non-uniform wave along the radial direction, then $Z_n(\gamma)$ in Eq. (23) can be written as:

$$Z_n(i\delta)=\frac{2K_n(\delta)}{K_{n-1}(\delta)+K_{n+1}(\delta)}; \tag{29}$$

where $K_z(\delta)$ is the improved Hankel function.

The radiation impedance Z_{nmm} represents the self-radiation impedance. When solving the infinite integral in the self-radiation impedance Eq. (23), it is found that the integrand has a high-order singularity. There are two singular points 1 and $m\pi/(k_cL)$ in the integrand expression. In order to accurately obtain the integral result, the integral interval is divided into small intervals according to the singular points, and the integral value is accumulated and calculated to obtain the theoretical calculation result of the acoustic radiation impedance.

Furthermore, according to the continuity boundary condition, Eq. (19) can be rewritten to obtain:

$$\begin{Bmatrix} U_{nma}^{\alpha} \\ V_{nma}^{\alpha} \\ W_{nma}^{\alpha} \\ F_{nma}^{\sigma z\alpha} \\ F_{nma}^{\sigma\phi\alpha} \\ F_{nma}^{\sigma r\alpha} \end{Bmatrix}=\begin{bmatrix} \mathbf{T}_{11} & \mathbf{T}_{12} \\ \mathbf{T}_{21} & \mathbf{T}_{22} \end{bmatrix}\begin{Bmatrix} U_{nmb}^{c\alpha} \\ V_{nmb}^{c\alpha} \\ W_{nmb}^{c\alpha} \\ 0 \\ 0 \\ i\omega Z_{nmm}W_{nmb}^{c\alpha} \end{Bmatrix}. \tag{30}$$

Decomposing Eq. (30) yields:

$$\begin{Bmatrix} U_{nma}^{\alpha} \\ V_{nma}^{\alpha} \\ W_{nma}^{\alpha} \end{Bmatrix}=(\mathbf{T}_{11}+\mathbf{T}_{12}\mathbf{A})\begin{Bmatrix} U_{nmb}^{c\alpha} \\ V_{nmb}^{c\alpha} \\ W_{nmb}^{c\alpha} \end{Bmatrix}; \tag{31}$$

$$\begin{Bmatrix} F_{nma}^{\sigma z\alpha} \\ F_{nma}^{\sigma\phi\alpha} \\ F_{nma}^{\sigma r\alpha} \end{Bmatrix}=(\mathbf{T}_{21}+\mathbf{T}_{22}\mathbf{A})\begin{Bmatrix} U_{nmb}^{c\alpha} \\ V_{nmb}^{c\alpha} \\ W_{nmb}^{c\alpha} \end{Bmatrix}; \tag{32}$$

where matrix $\mathbf{A}=\begin{bmatrix} 0 & 0 & 0 \\ 0 & 0 & 0 \\ 0 & 0 & i\omega Z_{nmm} \end{bmatrix}$, inverting Eq. (31) and substituting it into Eq. (32) yields:

$$\begin{Bmatrix} F_{nma}^{\sigma z\alpha} \\ F_{nma}^{\sigma\phi\alpha} \\ F_{nma}^{\sigma r\alpha} \end{Bmatrix}=(\mathbf{T}_{21}+\mathbf{T}_{22}\mathbf{A})(\mathbf{T}_{11}+\mathbf{T}_{12}\mathbf{A})^{-1}\begin{Bmatrix} U_{nma}^{\alpha} \\ V_{nma}^{\alpha} \\ W_{nma}^{\alpha} \end{Bmatrix}; \tag{33}$$

$$\begin{Bmatrix} -F_{nma}^{\sigma z\alpha} \\ -F_{nma}^{\sigma\phi\alpha} \\ F_{nma}^{\sigma r\alpha} \end{Bmatrix}=\mathbf{B}\begin{Bmatrix} F_{nma}^{\sigma z\alpha} \\ F_{nma}^{\sigma\phi\alpha} \\ F_{nma}^{\sigma r\alpha} \end{Bmatrix}= \mathbf{B}(\mathbf{T}_{21}+\mathbf{T}_{22}\mathbf{A})(\mathbf{T}_{11}+\mathbf{T}_{12}\mathbf{A})^{-1}\begin{Bmatrix} U_{nma}^{\alpha} \\ V_{nma}^{\alpha} \\ W_{nma}^{\alpha} \end{Bmatrix}; \tag{34}$$

where matrix $\mathbf{B} = \begin{bmatrix} -1 & 0 & 0 \\ 0 & -1 & 0 \\ 0 & 0 & -1 \end{bmatrix}$, substituting Eq. (34) into Eq. (6), we obtain:

$$\left(\begin{bmatrix} s_{11} & s_{12} & s_{13} \\ s_{21} & s_{22} & s_{23} \\ s_{31} & s_{32} & s_{33} \end{bmatrix} - \frac{\mathbf{B}(\mathbf{T}_{21}+\mathbf{T}_{22}\mathbf{A})(\mathbf{T}_{11}+\mathbf{T}_{12}\mathbf{A})^{-1}}{\rho_p c_p^2 h} \right) \cdot \begin{Bmatrix} U_{nma}^{\alpha} \\ V_{nma}^{\alpha} \\ W_{nma}^{\alpha} \end{Bmatrix} = \frac{1}{\rho_p c_p^2 h} \begin{Bmatrix} 0 \\ 0 \\ F_{nm}^{\alpha} \end{Bmatrix}. \quad (35)$$

The above equation is the motion equation of the cylindrical shell with anisotropic mechanical material under fluid-solid coupling. Solving Eq. (35) can obtain the radial displacement W_{nma}^{α} of the cylindrical shell with anisotropic mechanical material.

The radiated sound power can be expressed as:

$$p(\omega) = \frac{1}{2} \int_0^{2\pi} a \, d\varphi \int_0^{L} \mathrm{Re}\left(p(a,\varphi,z)\dot{\omega}^*(\varphi,z)\right) dz = \frac{S}{4} \mathrm{Re}\left(\sum_{n=0}^{\infty} \sum_{m=1}^{\infty} \dot{W}_{nm} Z_{nmm} \dot{W}_{nm}^* \right); \quad (36)$$

in which, "*" represents a conjugate complex number and S is the surface area of the shell. The sound power level is used to measure the sound radiation performance and is defined as:

$$L_w = 10 \log \frac{p(\omega)}{1 \times 10^{-12}}. \quad (37)$$

Substituting the radial displacement W_{nma}^{α} of the cylindrical shell with anisotropic mechanical material obtained in the previous section into Eqs. (36) and (37), the radiated sound power level can be obtained, and then the acoustic vibration characteristics of the cylindrical shell with anisotropic mechanical material can be analyzed.

3. CONFORMANCE VERIFICATION

Traditional methods usually ignore the effect of shear waves and model mechanical materials as fluids. In order to further verify the effectiveness of laying anisotropic mechanical material cylindrical shells, an analytical model of the acoustic vibration characteristics of isotropic mechanical material cylindrical shells based on fluid equivalence was first established and compared with the numerical model. It is easy to find that the acoustic field in the external fluid satisfies the Helmholtz equation:

$$\nabla^2 p_0 + \kappa_0^2 p_0 = 0; \quad (38)$$

in which $\kappa_0 = \omega/c_0$, c_0 is the fluid sound velocity.

The acoustic field in mechanical materials also satisfies the Helmholtz equation:

$$\nabla^2 p + \kappa_t^2 p = 0; \quad (39)$$

in which $\kappa_t = \omega/c_t$, c_t is the longitudinal wave velocity in mechanical materials. The thickness and length of mechanical materials are limited, and standing waves are formed in the radial direction, which can be expressed by a combination of Bessel functions. The mode in the axial direction should be the same as the shell mode, so the formal solution of the acoustic field in the mechanical material can be written as:

$$p_1(z,\theta,r) = \sum_{\alpha,n,m} p_{nm,1}(r) \sin\left(n\theta + \frac{\alpha\pi}{2}\right) \sin\frac{m\pi z}{L}; \quad (40)$$

where:

$$p_{nm,1}(r) = A_{n,1} J_n(k_t r) + B_{n,1} Y_n(k_t r); \quad (41)$$

in which $k_t^2 = \kappa_t^2 - k_m^2$, $\kappa_t = \omega/c_t$, $k_m = m\pi/L$, J_n and Y_n are the first and second kind of Bessel functions respectively, and $A_{n,1}$ and $B_{n,1}$ are the coefficients to be determined.

Similarly, the acoustic pressure at the interface between the mechanical material and the external fluid can be expanded as follows:

$$p_0(z,\theta,b) = \sum_{\alpha,n,m} p_{nm,0}(r) \sin\left(n\theta + \frac{\alpha\pi}{2}\right) \sin\frac{m\pi z}{L}; \quad (42)$$

where:

$$p_{nm,0} = \dot{W}_{nm}^b Z_{nmm}; \quad (43)$$

in which $\dot{W}_{nm}^b$ is the vibration velocity of the outer surface of the mechanical material. The superscript b represents the outer surface radius of the mechanical material. Z_{nmm} is the self-radiation impedance of the corresponding mode, where the mutual radiation impedance is neglected.

According to the equation of motion, the acoustic pressure $p_{nm,0}$ on the surface of a mechanical material can be written as:

$$p_{nm,0} = \frac{1}{i\omega\rho_1} \frac{\partial p_{nm,1}(r)}{\partial r}\bigg|_{r=b} Z_{nmm}. \quad (44)$$

The boundary conditions between the mechanical material and the external fluid and between the mechanical material and the shell are as follows: First, the sound pressure and vibration velocity are continuous at the interface between the external fluid and the mechanical material at $r = b$. Second, the vibration velocity is continuous at the interface between the mechanical material and the shell at $r = a$, and the sound pressure is equal to the reaction pressure p_c of the mechanical material on the shell. Then:

$$\begin{aligned} r = b, \quad & p_{nm,0}(r) = p_{nm,1}(r); \\ & \frac{1}{i\omega\rho_0} \frac{\partial p_{nm,0}(r)}{\partial r} = \frac{1}{i\omega\rho_1} \frac{\partial p_{nm,1}(r)}{\partial r}; \\ r = a, \quad & \dot{W}_{nm}^a = \frac{1}{i\omega\rho_M} \frac{\partial p_{nm,M}(r)}{\partial r}. \end{aligned} \quad (45)$$

Substituting the sound pressure solution into the boundary condition Eq. (45) we can obtain:

$$\begin{aligned} & A_{n,1} T_{11} + B_{n,1} T_{12} = 0; \\ & A_{n,M} T_{21} + B_{n,M} T_{22} = -i\omega W_{nm}^a; \end{aligned} \quad (46)$$

where:

$$\begin{aligned} T_{11} &= \frac{k_1}{i\omega\rho_1} J_n'(k_1 b) Z_{nm}^A - J_n(k_1 b); \\ T_{12} &= \frac{k_1}{i\omega\rho_1} Y_n'(k_1 b) Z_{nm}^A - Y_n(k_1 b); \\ T_{21} &= \frac{k_M}{i\omega\rho_M} J_n'(k_M a); \\ T_{22} &= \frac{k_M}{i\omega\rho_M} Y_n'(k_M a). \end{aligned} \quad (47)$$

Table 1. Material properties and geometric dimensions of the cylindrical shell model.

	Material	Length (m)	Radius (m)	Thickness(m)	Density (kg/m^3)	Young's modulus (Pa)	Poisson's ratio	Damping
Shell	Steel	3.8	1.2	0.008	7800	2.1e11	0.3	0.001

Table 2. Mechanical material parameters / (1×10^7) Pa.

E_{11}	E_{22}	E_{33}	G_{12}	G_{23}	G_{31}	ν_{21}	ν_{31}	ν_{32}
3.53	2.49	1.89	1.15	1.18	1.12	0.24	0.31	0.59

This produces the system of equations:

$$\begin{bmatrix} T_{11} & T_{12} \\ T_{21} & T_{22} \end{bmatrix} \begin{Bmatrix} A_{n,M} \\ B_{n,M} \end{Bmatrix} = \begin{Bmatrix} 0 \\ -i\omega W_{nm}^a \end{Bmatrix}. \tag{48}$$

The above equation is used to solve the unknown coefficients $A_{n,M}$, $B_{n,M}$ for the shell surface displacement W_{nm}^a. According to the formal solution of the sound pressure in the mechanical material, the following relationship is further obtained:

$$\begin{aligned} p_{nm,1} &= \frac{i\omega}{\Delta_T} \left[T_{12} J_n(k_1 a) - T_{11} Y_n(k_1 a) \right] W_{nm}^a; \\ \dot{W}_{nm}^b &= \frac{k_1}{\rho_1 \Delta_T} \left[T_{12} J_n'(k_1 b) - T_{11} Y_n'(k_1 b) \right] W_{nm}^a; \end{aligned} \tag{49}$$

where Δ_T is the determinant value of the coefficient matrix in Eq. (48). Substituting the radial displacement of the cylindrical shell with isotropic mechanical materials into Eqs. (36) and (37), the radiated sound power and radial mean square velocity can be obtained, which allows for the acoustic vibration characteristics of the cylindrical shell with isotropic mechanical materials to be analyzed.

Furthermore, a finite element numerical model was established and the acoustic-vibration characteristics were compared with those obtained by two analytical methods. In general, the stiffness matrix of an elastic material can be written as:

$$[C_{ij}] = \begin{bmatrix} C_{11} & C_{12} & C_{13} & 0 & 0 & 0 \\ C_{12} & C_{22} & C_{23} & 0 & 0 & 0 \\ C_{13} & C_{23} & C_{33} & 0 & 0 & 0 \\ 0 & 0 & 0 & C_{44} & 0 & 0 \\ 0 & 0 & 0 & 0 & C_{55} & 0 \\ 0 & 0 & 0 & 0 & 0 & C_{66} \end{bmatrix}. \tag{50}$$

In the formula, the 1st, 2nd, and 3rd principal directions of the stiffness matrix correspond to the radial r, circumferential ϕ, and axial z directions of the mechanical material. The stiffness matrix is converted into the flexibility matrix and the parameter transformation relationship is given as:

$$[S_{ij}] = \begin{bmatrix} \frac{1}{E_{11}} & -\frac{\nu_{21}}{E_{22}} & -\frac{\nu_{31}}{E_{33}} & 0 & 0 & 0 \\ -\frac{\nu_{12}}{E_{11}} & \frac{1}{E_{11}} & -\frac{\nu_{32}}{E_{33}} & 0 & 0 & 0 \\ -\frac{\nu_{13}}{E_{11}} & -\frac{\nu_{23}}{E_{22}} & \frac{1}{E_{33}} & 0 & 0 & 0 \\ 0 & 0 & 0 & \frac{1}{G_{23}} & 0 & 0 \\ 0 & 0 & 0 & 0 & \frac{1}{G_{31}} & 0 \\ 0 & 0 & 0 & 0 & 0 & \frac{1}{G_{12}} \end{bmatrix}; \tag{51}$$

$$\begin{aligned} C_{11} &= \frac{1 - \nu_{23}\nu_{32}}{E_{22}E_{33}\Delta}; \\ C_{12} &= \frac{\nu_{21} + \nu_{31}\nu_{23}}{E_{22}E_{33}\Delta} = \frac{\nu_{12} + \nu_{32}\nu_{13}}{E_{11}E_{33}\Delta}; \\ C_{13} &= \frac{\nu_{31} + \nu_{21}\nu_{32}}{E_{22}E_{33}\Delta} = \frac{\nu_{13} + \nu_{12}\nu_{23}}{E_{11}E_{22}\Delta}; \\ C_{22} &= \frac{1 - \nu_{13}\nu_{31}}{E_{11}E_{33}\Delta}; \\ C_{23} &= \frac{\nu_{32} + \nu_{12}\nu_{31}}{E_{11}E_{33}\Delta} = \frac{\nu_{23} + \nu_{21}\nu_{13}}{E_{11}E_{22}\Delta}; \\ C_{33} &= \frac{1 - \nu_{12}\nu_{21}}{E_{11}E_{22}\Delta}; \\ \Delta &= \frac{1 - \nu_{12}\nu_{21} - \nu_{23}\nu_{32} - \nu_{13}\nu_{31} - 2\nu_{21}\nu_{32}\nu_{13}}{E_{11}E_{22}E_{33}}. \end{aligned} \tag{52}$$

Given the tensile modulus, Poisson's ratio and shear modulus of the material, the stiffness matrix of the elastic material can be calculated according to Eq. (52). Furthermore, analytical and numerical methods were used to calculate the radiated sound power of the cylindrical shell covered with anisotropic mechanical materials, respectively, to verify the effectiveness of the analytical model of acoustic-vibration characteristics. Table 1 gives the material properties and geometric dimensions of the cylindrical shell model, and the material parameters of the mechanical material are shown in Table 2. Among them, the mechanical material is the same length as the cylindrical shell, the density is 971.2339 kg/m^3, the thickness is 0.02 m, and the loss factor is set to 0.25.

A numerical model of a cylindrical shell with anisotropic mechanical materials is established, as shown in Fig. 2. The structure is immersed in an infinite water area. The material properties and geometric parameters of the cylindrical shell and mechanical materials are shown in Tables 1 and 2, where the rigid cylindrical baffles connected at both ends of the shell are of the same length as the shell and have the same material properties as the shell. The shell is modeled using shell elements, and the mechanical material and rigid cylindrical baffles are modeled using solid elements. Simply supported boundary conditions are applied at both ends of the shell, and the vibration displacement of the rigid baffle is set to zero. The cylindrical shell is immersed in water and a radial point excitation force is applied in the middle of the shell surface. A perfectly matched layer (PML) boundary condition is applied at the outer boundary of the fluid domain to simulate the anechoic termination of the output wave.

For uniform mechanical materials, when the frequency is low, the longitudinal wave effect is the main one. At this time, the mechanical material can be approximately regarded as a fluid, that is, the effect of shear waves can be ignored. In fact, the mechanical material has interaction forces on the cylindrical shell in the radial, circumferential and axial directions. Therefore, the acoustic and vibration characteristics of isotropic mechanical materials based on fluid equivalence and anisotropic mechanical materials based on state space vectors are compared here. The radiated sound power of the cylindrical shell coated with mechanical materials under fluid-solid coupling is solved by analytical and numerical models. The

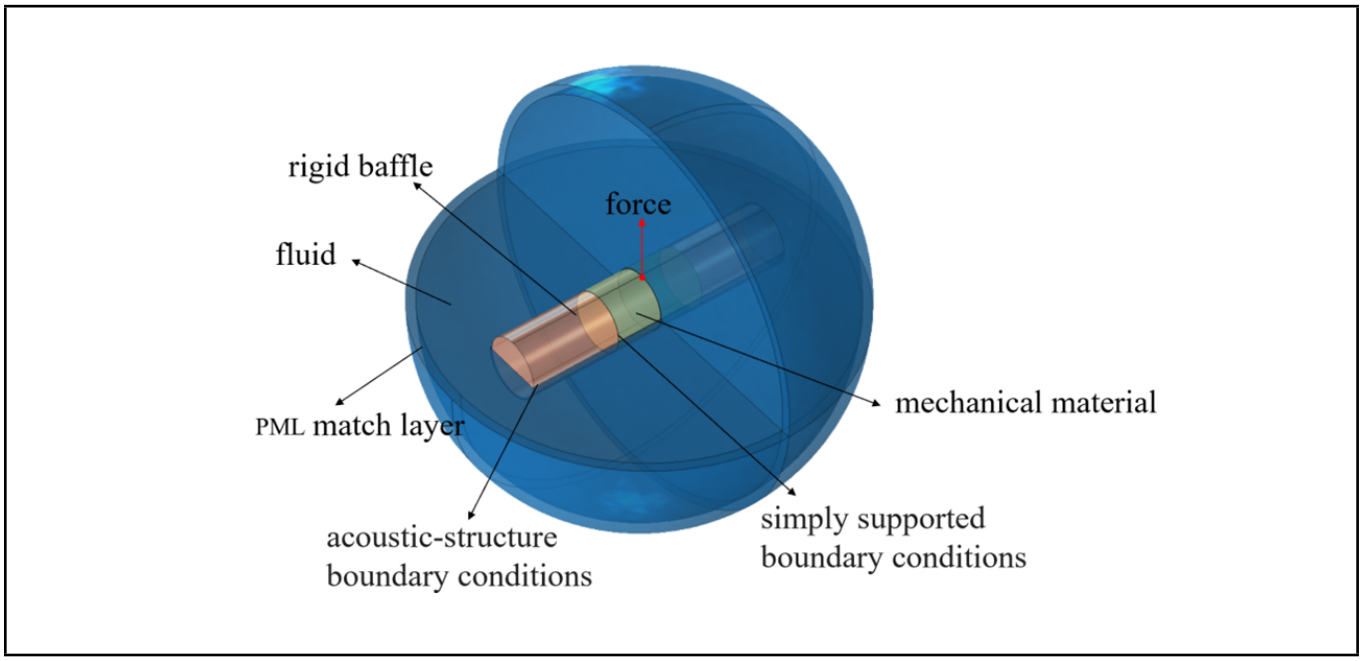

Figure 2. The model for laying anisotropic mechanical material cylindrical shell.

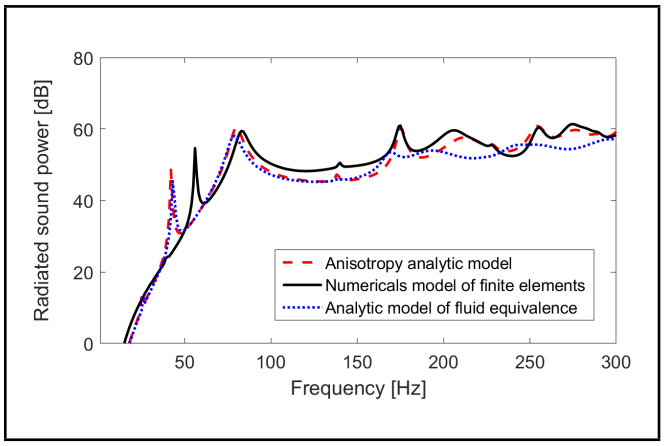

Figure 3. Verification of the accuracy of the shell modeling method.

results are shown in Fig. 3. Among them, the black solid line represents the numerical solution of the cylindrical shell with anisotropic mechanical material calculated using the finite element method, the red dotted line represents the analytical solution of the anisotropic mechanical material based on the state space vector, and the blue dotted line represents the radiated sound power of the analytical model of the isotropic mechanical material obtained based on fluid equivalence.

As can be seen from Fig. 3, the equivalent of the anisotropic mechanical material shell based on the state space is closer to the finite element result and has higher accuracy. However, due to the influence of boundary conditions in theory and simulation and the neglect of the influence of mutual radiation, there are certain errors in the theoretical and simulation results in the entire frequency band. Overall, the analytical model of the cylindrical shell with anisotropic mechanical materials can reflect its true characteristics and can be used for subsequent analysis and prediction of the transmission law of radiation noise of the cylindrical shell with anisotropic mechanical materials.

4. REGULAR ANALYSIS

4.1. Mechanical Material Parameters Are Negative

By introducing the design concept of metamaterials, the material properties of the laying layer are designed to be material parameters that can produce negative properties. Elastic waves become evanescent waves that cannot propagate in the frequency range of negative numbers. The influence of negative mechanical material parameters on the radiation noise characteristics of cylindrical shells of laying anisotropic mechanical materials is further analyzed. The material parameters in Table 2 are selected as the original parameters, among which the three tensile moduli are radial, circumferential, and axial tensile moduli, corresponding to E_{11}, E_{22}, and E_{33}, and the three shear moduli are the shear moduli in the $r\phi$, ϕz, and zr directions, corresponding to G_{12}, G_{23}, and G_{31}. After changing the tensile modulus parameters, the material parameters that produce negative properties can be expressed as:

$$E_p = E_0 \frac{-\omega^2 + \omega_z^2}{-\omega^2 + \omega_p^2}, \qquad \omega_p = 2\pi f_p. \tag{53}$$

In the formula, E_p and E_0 represent the negative material parameters and original parameters after design, respectively, $\omega_p 0$ and ω_z are poles and zeros, respectively, and the two satisfy the relationship: $\omega_z < \omega_p$. f_p is the regulating factor of the material parameters, and its physical meaning represents the resonant frequency.

Before applying negative material parameters to analyze the transmission characteristics of elastic waves, the control law of the regulating factor on the negative material parameters is first analyzed. Taking the circumferential tensile modulus E_{22} as an example, the control law of the regulating factor f_p on the designed negative material parameter E_{22p} is studied, as shown in Fig. 4.

Figure 4 shows the variation of the tensile modulus E_{22p} with the control factor f_p. It can be found that the tensile mod-

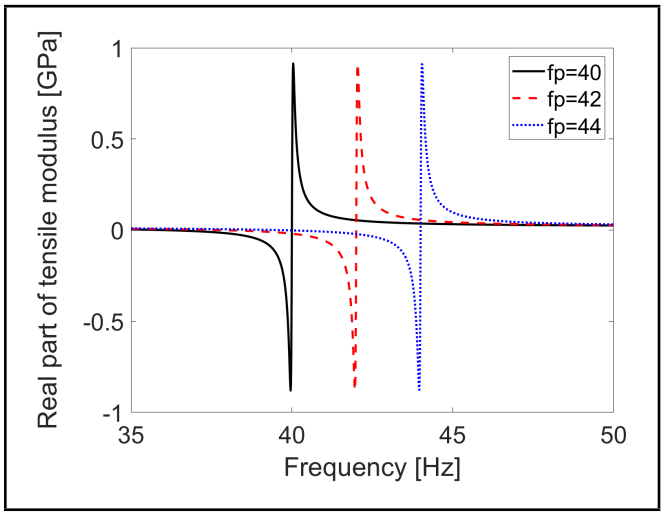

Figure 4. Changes of the real part of the tensile modulus with the control factor f_p.

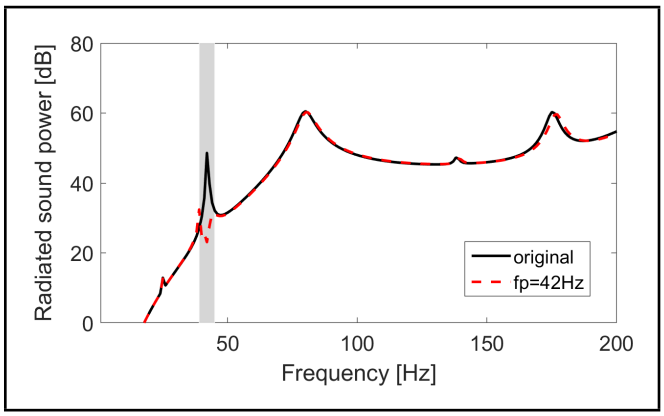

Figure 5. Effect of introducing negative material parameter E_{22p} on radiated sound power.

ulus produces a resonance effect at the frequency corresponding to the control factor f_p and a negative region appears within a certain frequency range. By changing the control factor f_p, the resonance effect of the real part of the tensile modulus and the negative attribute region appear at the corresponding frequency position.

The circumferential tensile modulus E_{22} of the mechanical material is designed as the negative material parameter E_{22p}, and the comparison results of the radiated sound power of the cylindrical shell laid with anisotropic mechanical material when the circumferential tensile modulus is E_{22p} and E_{22} respectively are obtained, as shown in Fig. 5.

As can be seen from Fig. 5, when the material parameters of the mechanical material are designed to be negative, the radiated sound power of the cylindrical shell laid with anisotropic mechanical materials is significantly reduced within the target frequency band. This phenomenon can be explained by the influence of negative material parameters on elastic waves: by analogy with the concept of metamaterials, the material parameters are designed to be negative, and the imaginary part of the elastic wave is not zero within the target frequency band, that is, an evanescent wave. At this time, the elastic wave generated by the structural vibration cannot propagate outward, which significantly reduces the radiated sound power of the cylindrical shell.

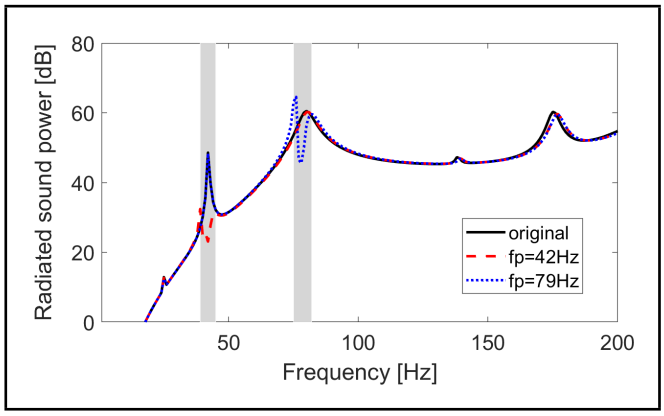

Figure 6. Radiated sound changes with the negative material parameter E_{22p} control factor f_p.

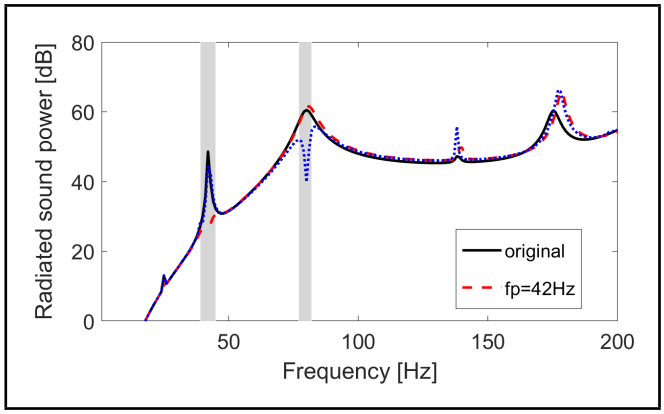

Figure 7. Radiated sound changes with the negative material parameter E_{11p} control factor f_p.

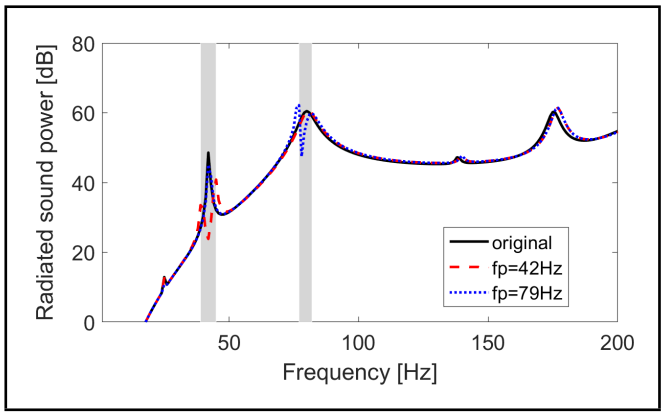

Figure 8. Radiated sound changes with the negative material parameter E_{33p} control factor f_p.

Next, the influence of the control factor f_p of the negative material parameter of the mechanical material on the radiated sound power was further analyzed. The control factor f_p was set to 42 Hz, 79 Hz, and 173 Hz for the resonance frequency of the radiated sound power, and the corresponding radiated sound power results were obtained, as shown in Fig. 6. Without loss of generality, the radial and axial tensile moduli E_{11} and E_{33} in the mechanical material were also designed as negative parameters, and the radiated sound power curves of the cylindrical shell at different control factors f_p were obtained, as shown in Figs. 7 and 8.

It can be seen from Fig. 6 that by setting the negative ma-

terial parameter control factor f_p at the target frequency, the bandgap generated by the negative parameter can effectively reduce the radiated sound power. The same conclusion can be drawn from Figs. 7 and 8. By designing the radial tensile modulus and axial tensile modulus in the material parameters to negative numbers, the radiated sound power in the frequency range corresponding to the control factor f_p can be significantly reduced, achieving effective suppression of radiated noise.

4.2. Mechanical Material Parameters Are Complex Numbers

When the material parameters are designed as negative numbers, a bandgap can be generated at the target frequency and the propagation of elastic waves can be effectively suppressed, thereby achieving the effect of reducing the radiated sound power. However, although this method can effectively reduce the radiated noise of the target frequency, it will produce higher secondary resonance peaks on both sides of the frequency, thereby weakening the suppression effect of the radiated noise. Considering that in the analysis of the influence of material parameters on the characteristics of elastic waves, the resonance intensity near the target frequency can be mitigated by designing it as a complex number. Therefore, considering designing the material parameters of the mechanical material as a complex number, that is, introducing the control factor β, and further analyzing the influence of the control factor β on the radiated sound power, the material parameters of the mechanical material can be further written in the form of a complex number, expressed as:

$$E_p = E_0 \frac{-\omega^2 + 2i\beta\omega_z\omega + \omega_z^2}{-\omega^2 + 2i\beta\omega_p\omega + \omega_p^2}, \qquad \omega_p = 2\pi f_p; \tag{54}$$

in which β is the newly introduced control factor of material parameters, and its physical meaning is expressed as loss factor.

Similarly, taking the circumferential tensile modulus E_{22} as an example, the control law of the regulation factor β on the designed composite material parameter E_{22p} is studied, as shown in Fig. 9.

Figure 9 shows the variation of the tensile modulus E_{22p} with the control factor β. At this time, $f_p = 42$ Hz remains constant. It can be found that as the control factor β increases, the resonance effect in the real part of the tensile modulus gradually weakens, which is manifested as the resonance peak changes from sharp to gentle. In addition, the peak value of the imaginary part of the tensile modulus also gradually decreases, and its non-zero range gradually widens.

Therefore, the circumferential tensile modulus E_{22} of the mechanical material is designed as a complex number, and the comparative results of the radiated sound power of the cylindrical shell when the circumferential tensile modulus has different regulation factors β are analyzed, as shown in Fig. 10.

As can be seen from Fig. 10, by increasing the complex material parameter control factor β, although the trough of the radiated sound power generated by the bandgap at the target frequency has a certain increase, the secondary resonance peaks generated on both sides of the frequency have been significantly reduced, and the overall control effect of the radiated sound power of the cylindrical shell laid with anisotropic mechanical materials has been improved.

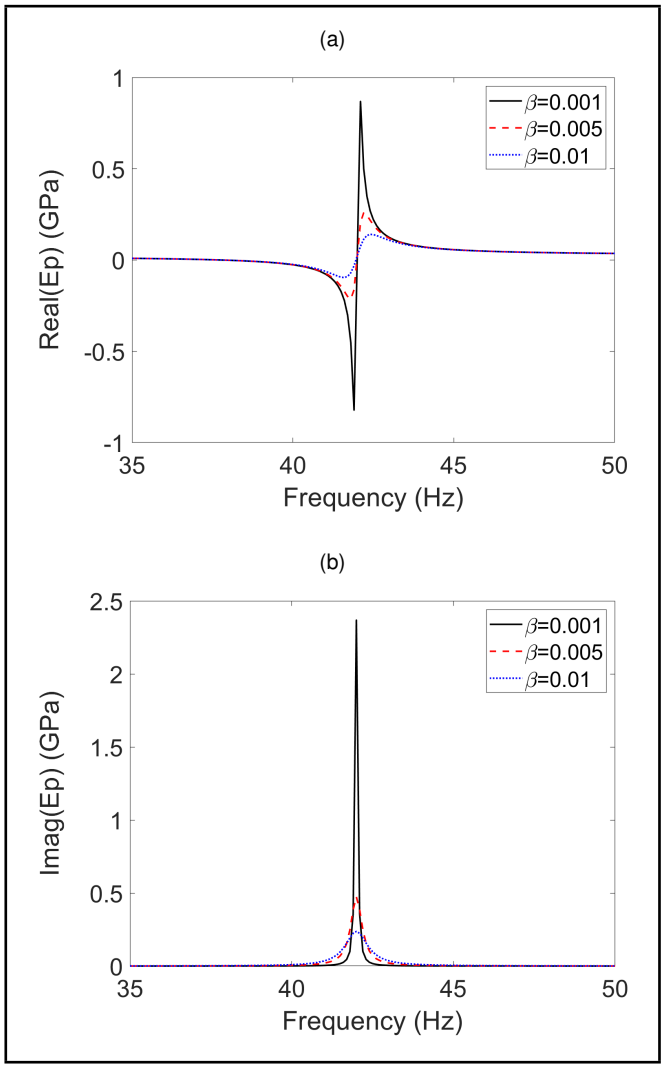

Figure 9. Changes of tensile modulus with control factor β: (a) real part and (b) imaginary part.

Similarly, the radial tensile modulus E_{11} and the axial tensile modulus E_{33} of the mechanical material are designed as complex numbers, and the cylindrical shell radiated sound power curves corresponding to different control factors β are obtained, as shown in Figs. 11 and 12.

It can be seen from Figs. 11 and 12 that by designing the radial and axial tensile moduli as complex numbers and increasing the control factor β, the secondary resonance peaks on both sides of the target frequency can be reduced and the overall control effect of the radiated noise at the target frequency can be effectively improved.

The comprehensive research results show that by designing the radial, axial and circumferential tensile moduli in the material parameters as negative numbers, the radiated sound power in the frequency range corresponding to the control factor f_p can be significantly reduced, and the propagation of radiated noise in a specific frequency band can be controlled. After introducing β, the radial, axial and circumferential tensile moduli are designed to be complex numbers, which can reduce the newly generated secondary resonance peaks on both sides of the bandgap range and achieve effective suppression of the overall radiation noise.

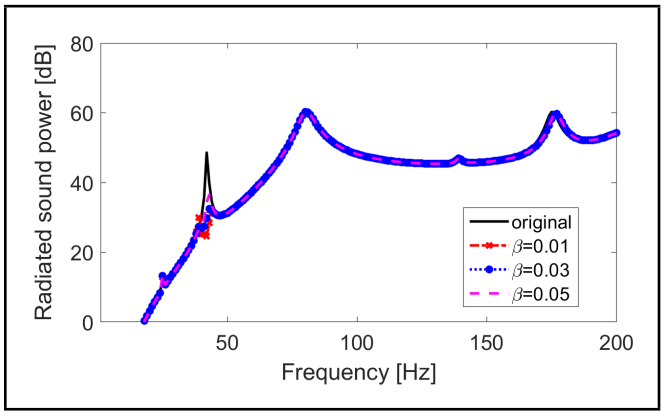

Figure 10. Radiated sound changes with the complex material parameter E_{22p} control factor β.

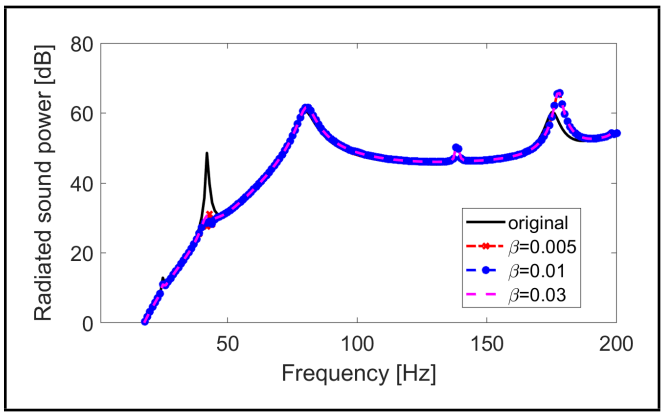

Figure 11. Radiated sound changes with the complex material parameter E_{11p} control factor β.

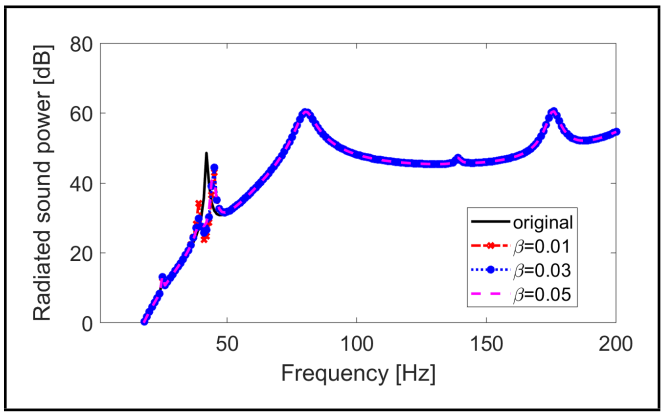

Figure 12. Radiated sound changes with the complex material parameter E_{33p} control factor β.

5. CONCLUSIONS

Based on three-dimensional elastic theory and state space vector method, this paper depicts a modeling method for the acoustic vibration characteristics of cylindrical shells with anisotropic mechanical materials. By analyzing the radiation noise characteristics of the finite element model and the analytical model, the accuracy of the theoretical solution of cylindrical shells with anisotropic mechanical materials was verified. Then, the material parameters of the mechanical material were changed to negative or complex numbers, and the influence on the radiation noise transfer characteristics was analyzed. Through the design of metamaterials, the method and mechanism of achieving low-frequency vibration and noise reduction of cylindrical shells were revealed, which provides guidance for the further design of adjustable mechanical materials.

REFERENCES

[1] Lin, Y. N. and Tucker, A. J. The distribution of radiated and vibratory powers of appoint-infinite cylindrical shell with a compliant layer, *INTER-NOISE and NOISE-CON Congress and Conference Proceedings*, Indiana, (1988).

[2] Laulagnet, B. and Guyader, J. L. Sound radiation from a finite cylindrical shell covered with a compliant layer, *Journal of Vibration and Acoustics*, **113**, 267–272, (1991). https://doi.org/10.1115/1.2930180

[3] Laulagnet, B. and Guyader, J. L. Sound radiation from finite cylindrical shell, partially coated with longitudinal strip of compliant layer, *Journal of Vibration and Acoustics*, **186** (5), 723–742, (1995). https://doi.org/10.1006/jsvi.1995.0485

[4] Cuschieri, J. M. and Feit, D. Influence of circumferential partial coating on the acoustic radiation from a fluid-loaded shell, *The Journal of the Acoustical Society of America*, **107** (6), 3196–3207, (2000). https://doi.org/10.1121/1.429347

[5] Heil, M., Kharrat, T., Cotterill, P. A., and Abrahams, I. D. Quasi-resonances in sound-insulating coatings, *Journal of Sound and Vibration*, **331** (21), 4774–4784, (2012). https://doi.org/10.1016/j.jsv.2012.05.029

[6] Laulagnet, B. and Guyader, J. L. Sound radiation from finite cylindrical coated shells, by means of asymptotic expansion of three-dimensional equations for coating, *The Journal of the Acoustical Society of America*, **96** (1), 277–286, (1994). https://doi.org/10.1121/1.410480

[7] Haifeng, A., Zhijian, C., and Qian, S. Acoustic design technology for reducing low-frequency noise of double-layer stiffened cylindrical shells (in Chinese), *Noise and Vibration Control*, **2007** (03), 106–109, (2007). https://doi.org/10.3969/j.issn.1006-1355.2007.03.028

[8] Xia, Q. and Chen, Z. Acoustic-vibration characteristics of ring-stiffened cylindrical shells based on structural reinforcement technology (in Chinese), *Journal of Huazhong University of Science and Technology (Natural Science Edition)*, **40** (01), 90–94, (2012).

[9] Shen, S., Leng, W., and Cheng, G. Study on vibration transmission and acoustic radiation of multi-layer vibration isolation system with composite structure (in Chinese), *Ship Mechanics*, **2** (002), 49–60, (1997).

[10] Cao, Y., Sun, H., An, F., and Li, X. Active control of low-frequency sound radiation by cylindrical shell with piezoelectric stack force actuators, *Journal of Sound and Vibration*, **331** (11), 2471–2484, (2012). https://doi.org/10.1016/j.jsv.2012.02.001